

This is an Open Access document downloaded from ORCA, Cardiff University's institutional repository: <https://orca.cardiff.ac.uk/id/eprint/101646/>

This is the author's version of a work that was submitted to / accepted for publication.

Citation for final published version:

Malhotra, Shashwat, Singh, Seema, Rana, Neha, Tomar, Shilpi, Bhatnagar, Priyanka, Gupta, Mohit, Singh, Suraj K., Singh, Brajendra K., Chhillar, Anil K., Prasad, Ashok K., Len, Christophe, Kumar, Pradeep, Gupta, Kailash C., Varma, Anjani J., Kuhad, Ramesh C., Sharma, Gaimda L., Parmar, Virinder S. and Richards, Nigel 2017. Chemoenzymatic synthesis, nanotization and anti- aspergillus activity of optically enriched fluconazole analogues. *Antimicrobial Agents and Chemotherapy* 61 (8) , e00273-17. 10.1128/AAC.00273-17

Publishers page: <http://dx.doi.org/10.1128/AAC.00273-17>

Please note:

Changes made as a result of publishing processes such as copy-editing, formatting and page numbers may not be reflected in this version. For the definitive version of this publication, please refer to the published source. You are advised to consult the publisher's version if you wish to cite this paper.

This version is being made available in accordance with publisher policies. See <http://orca.cf.ac.uk/policies.html> for usage policies. Copyright and moral rights for publications made available in ORCA are retained by the copyright holders.



27 **Abstract**

28 Despite recent advances in diagnostic and therapeutic advances in antifungal
29 research, aspergillosis still remains a leading cause of morbidity and mortality. One
30 strategy to address this problem is to enhance the activity spectrum of known
31 antifungals, and we now report the first successful application of *Candida antarctica*
32 lipase (CAL) for the preparation of optically enriched fluconazole analogs. Anti-
33 *Aspergillus* activity was observed for an optically enriched derivative, (-)-*S*-2-(2',4'-
34 difluorophenyl)-1-hexyl-amino-3-(1''',2''',4''') triazol-1'''-yl-propan-2-ol, which exhibits
35 MIC values of 15.6 µg/mL and 7.8 µg/disc in microbroth dilution and disc diffusion
36 assays, respectively. This compound is tolerated by mammalian erythrocytes and
37 cell lines (A549 and U87) at concentrations of up to 1000 µg/mL. When incorporated
38 into dextran nanoparticles, the novel, optically enriched fluconazole analog exhibited
39 improved antifungal activity against *Aspergillus fumigatus* (MIC = 1.63 µg/mL).
40 These results not only demonstrate the ability of biocatalytic approaches to yield
41 novel, optically enriched fluconazole derivatives but also suggest that
42 enantiomerically pure fluconazole derivatives, and their nanotised counterparts,
43 exhibiting anti-*Aspergillus* activity may have reduced toxicity.

44 Aspergillosis remains a significant threat to public health, and, in spite of
45 continuous efforts to improve timely diagnosis and clinical therapies, mortality
46 caused by this disease remains unacceptably high [1, 2]. Current therapeutic
47 options for treating *Aspergillus*-induced disorders include antifungal agents
48 such as polyenes, azoles and echinocandins [3, 4]. Thus the discovery of new
49 antifungal compounds remains important given the need to address the
50 development of drug resistance in pathogenic fungi [5-7]. One approach to
51 accomplishing this goal is to prepare new derivatives of existing drugs with
52 broad spectrum activity and enhanced pharmacokinetic properties. As part of
53 our on-going efforts to use lipases [8-12], which catalyze reactions with high
54 degree of chemo-, regio- and stereoselectivity in organic synthesis, we
55 became interested in preparing new antifungals using biocatalysis.

56 Fluconazole, introduced in 1990, is a bis-triazole antifungal drug which
57 possesses interesting pharmacokinetic properties, such as low plasma binding
58 affinity, good water solubility, low first pass metabolism, high oral
59 bioavailability and a long half-life, all of which should make it a drug of choice
60 for treating fungal infections [13, 14]. On the other hand, fluconazole has been
61 reported to exhibit only limited activity against *Aspergillus* infections [15],
62 which has led to many reports concerning the synthesis of various types of
63 fluconazole derivatives and their chiral separation/resolution into constituent
64 enantiomers [16-19]. We now report the use of *Candida antarctica* lipase
65 (CAL-B) in catalysing the addition of amines to an achiral epoxide to yield
66 optically enriched fluconazole analogues in which one of the triazole rings is
67 replaced by *n*-alkylamino and cycloalkylamino substituents. To the best of our
68 knowledge, the work reported herein is the first direct synthesis of optically

69 enriched fluconazole analogues using biocatalytic methods. *In vitro* assays
70 show that the optically enriched analogues exhibit more potent antifungal
71 activity than the corresponding racemic mixtures. Interestingly, this bioactivity
72 can be enhanced by their encapsulation in dextran-based nanoparticles [20].

73

74 Results

75 **Synthesis of fluconazole analogues.** A series of linear and cyclic alkylamines
76 was screened for reaction with the epoxide ring of (\pm)-1-[2-(2, 4-difluorophenyl)-
77 oxiranylmethyl]-1*H*-[1,2,4]-triazole (**1**, Figure 1) in a number of different organic
78 solvents. Three different immobilized lipases were also evaluated for their ability to
79 catalyze this reaction: *Candida rugosa* lipase (CRL), porcine pancreatic lipase (PPL)
80 and CAL-B. Although the ring-opening reactions catalysed by CRL and PPL were of
81 no practical utility, when the reaction was performed in the presence of CAL-B in
82 tetrahydrofuran (THF) as solvent, the desired products (**3a-j**, **5a** and **5b**) were
83 obtained with good yields in optically enriched forms (Figure 1, and Tables S1 and
84 S2 in Supporting Information). Very importantly, all of the twelve novel fluconazole
85 analogues formed in the lipase-catalyzed reactions were optically active showing
86 that aminolysis of the racemic starting epoxide (\pm)-**1** had proceeded in an
87 enantioselective fashion (Table S1). These twelve compounds could also be
88 prepared in racemic form, as viscous oils in 75-80 % yields, by direct reaction of the
89 alkylamines with the racemic epoxide precursor (\pm)-**1** in THF at 55 °C. The time
90 taken for complete consumption of aliphatic amines **2a-j**, **4a** and **4b** in the CAL-B
91 catalyzed reaction varied between 18h and 28h, which was considerably shorter
92 than the 48-56 h required for the chemical addition of the amines (Table S2 in
93 Supporting Information). The structures of all twelve fluconazole analogues were

94 unambiguously established on the basis of spectroscopic data (IR, ^1H - and ^{13}C NMR,
95 and mass spectra), and by comparison to literature data for known compounds **3b**,
96 **3c**, **5a** and **5b** [21, 22].

97 Although the enantiomeric enrichment of the fluconazole analogues prepared
98 by lipase-catalyzed addition was not established, we were able to assign the
99 absolute configuration of the major enantiomer using the optical activity of the
100 unreacted epoxide isolated from the reaction mixture. These samples rotated
101 polarized light in a positive (+) direction, meaning that the recovered, unreacted
102 epoxide was enriched in the enantiomer for which the stereogenic centre has the (S)
103 configuration (Table S1 in Supporting Information) [23]. CAL-B therefore
104 preferentially employs (-)-*R*-**1** in the aminolysis reaction and, assuming a standard
105 $\text{S}_{\text{N}}2$ mechanism for reaction of the amine with the epoxide, we can deduce that the
106 fluconazole analogues must be enriched in the (-)-*S*-enantiomer (Figure 1).

107
108 **Antifungal activities of the fluconazole analogs** Pathogenic *Aspergillus*
109 strains (*Aspergillus fumigatus* ITCC 6604, *Aspergillus flavus* ITCC 5192, and
110 *Aspergillus niger* ITCC 0004) were used to determine the *in vitro* antifungal efficacy
111 of the fluconazole analogues, in both their optically enriched and racemic forms.
112 These experiments used standard microbroth dilution (MDA), disc diffusion (DDA)
113 and spore germination inhibition (PSGI) assays [24, 25]. We note that the MDA
114 assay is based on the same basic principle as that used in the CLSI micro-dilution
115 protocol. The only difference between the two assays is that CLSI uses RPMI
116 medium to prepare diluted drug solutions rather than the Sabouraud dextrose broth
117 (a medium used to culture *Aspergillus* in the laboratory) used by us to determine the
118 MIC of the fluconazole derivatives. As recommended in CLSI protocols, we carefully

119 monitored MDA parameters with respect to preparation of the test compounds,
120 medium preparation, temperature, inoculum size, incubation time, minimum
121 inhibitory concentration (MIC)/endpoint determination, data recording and
122 interpretation of results to ensure the validity and quality of our results. On this point,
123 we note that a previous study from our laboratory [26] showed that results with RPMI
124 1640 or RPMI 1640 containing glucose were not different from those obtained by
125 using Sabouraud dextrose broth.

126 On the basis of their MIC values, all the compounds exhibited moderate to
127 good anti-*Aspergillus* activities, with the analogue (-)-**S-3d** being more potent than
128 the commercially available fluconazole (Table 1). We also observed that optically
129 enriched mixtures of (-)-**S-3a**, (-)-**S-3c**, (-)-**S-3d**, (-)-**S-3e** and (-)-**S-5b** were more
130 active than the corresponding racemates. These data also confirm that introducing a
131 linear aliphatic alkyl side chain is important for imparting antifungal activity, as
132 reported previously [23, 24]. On the other hand, when additional, “distal” N-
133 substituted alkyl groups were present, as in compounds (-)-**S-3g** and (-)-**S-3h**,
134 antifungal activity was completely lost (Table 1). Compounds **3j** and **5a** exhibited no
135 biological activity in microbroth dilution assays and were not studied further. Our
136 work also shows that the length of the alkyl side chain is an important factor in
137 determining activity, i.e. the compound (-)-**S-3d**, containing an n-hexyl moiety, has
138 higher activity than (-)-**S-3a**, (-)-**S-3b** and (-)-**S-3c**, which contain ethyl, *n*-propyl and
139 *n*-butyl groups, respectively (Table 1). Decreasing the linker chain length also led to
140 higher activity. Optically enriched (-)-**S-3d** was the most potent compound against
141 *Aspergillus fumigatus* (Table 1) and was therefore used to examine how
142 encapsulation in dextran nanoparticles might impact anti-fungal activity.

143

144 **Characterization of (-)-S-3d release from O-alkylated dextran**
145 **nanoparticles.** Dextran nanoparticle-based drug delivery systems are
146 biocompatible, biodegradable, possess low immunogenicity [20], and can be used
147 for controlled release of pharmacologically active substances [27]. We therefore
148 encapsulated optically enriched (-)-S-3d into three types of dextran nanoparticles,
149 derivatized with O-hexadecyl, O-decyl and O-heptyl chains to ensure amphiphilicity,
150 and examined their effect on anti-*Aspergillus* activity. After trapping (-)-S-3d within
151 each of the nanoparticles by self-assembly (encapsulation efficiencies for the O-
152 hexadecyl, O-decyl and O-heptyl nanoparticles were 50 ± 4 %, 22 ± 2 % and 30 ± 2
153 %), the resulting particle size distributions were determined using dynamic light
154 scattering (DSL). These measurements showed that the sizes of the O-hexadecyl-,
155 O-decyl- and O-heptyl- derivatized nanoparticles were 140 ± 16 nm, 187 ± 13.16 nm
156 and 183 ± 14.73 nm, respectively, and that all of the samples had a low
157 polydispersity index (< 0.3) (Supporting Information). Examination of the rate at
158 which the fluconazole analogue (-)-S-3d was released from each of the three types
159 of nanoparticles, showed an initial burst for the O-hexadecyl- and O-decyl-
160 derivatized nanoparticles (Figure 2).

161

162 **Anti-*Aspergillus* activity and cytotoxicity of (-)-S-3d encapsulated in O-**
163 **alkylated dextran nanoparticles.** We next examined the effect of nanoparticle
164 encapsulation on the activity of (-)-S-3d against *Aspergillus fumigatus* using a
165 microbroth dilution assay (Figure 3). After 48 h of incubation (approximately 80 %
166 release), (-)-S-3d encapsulated in O-decyl-derivatized nanoparticles inhibited the
167 growth of *Aspergillus fumigatus* at an effective concentration of 3.16 $\mu\text{g/mL}$. Perhaps
168 more importantly, when the optically enriched fluconazole analogue was

169 encapsulated in *O*-hexadecyl nanoparticles, complete inhibition of *Aspergillus*
170 *fumigatus* growth was achieved at an effective concentration of 1.63 µg/mL (41.3 %
171 release at an initial concentration of 3.95 µg/mL). In addition, nanoparticle-
172 encapsulated (-)-**S-3d** exhibits activity at a lower concentration when compared to
173 both fluconazole and free (-)-**S-3d**. Although we believe that this effect is associated
174 with sustained release of the compound over time, it is also possible that drug
175 uptake is more efficient because the drug in its encapsulated form is more efficiently
176 captured by the cells. The general importance of this observation is also evident from
177 the fact that the MIC of amphotericin B was decreased from 1.95 µg/mL to 0.97
178 µg/mL when the drug was encapsulated in *O*-heptyl nanoparticles.

179 The cytotoxicity of (-)-**S-3d** and amphotericin B when encapsulated in
180 derivatized nanoparticles was also evaluated using haemolysis and MTT-based
181 assays (Figure 4). Perhaps unsurprisingly, given that erythrocytes and cell lines
182 treated with empty dextran nanoparticles (> 90 % cell viability at concentrations of 2
183 mg/mL) remained completely viable up to 1 mg/mL, the encapsulated, optically
184 enriched fluconazole analogue (-)-**S-3d** exhibited similar cytotoxicity to that of the
185 free compound. Thus, essentially no toxicity to two human cell lines (Figures 4b and
186 4c) was seen when the compound was present at concentrations similar to the MIC
187 values observed for its anti-fungal activity. The optically enriched fluconazole
188 analogue (-)-**S-3d** was also considerably less cytotoxic than free amphotericin B in
189 all assays (Figure 4). It is therefore interesting to note that encapsulating
190 amphotericin B into *O*-hexadecyl derivatized nanoparticles lowered the cytotoxicity of
191 this antifungal agent in both the hemolysis and MTT-based assays. Nevertheless,
192 cell viability was reduced for amphotericin B-containing nanoparticles relative to
193 derivatized nanoparticles containing fluconazole analogue (-)-**S-3d**.

Conclusions

Reacting alkylamines with a racemic epoxide precursor (Figure 1) in the presence of immobilized lipase CAL-B in THF provides a simple approach for the preparation of optically enriched fluconazole analogs, which appear to exhibit better antifungal activity against *Aspergillus* than fluconazole. Although the extent to which the enzyme catalyzes the coupling reaction in an enantioselective manner remains to be determined, we have been able to assign the (*S*)-configuration to the stereogenic centre of the enantiomer that exhibits biological activity, assuming that (i) the aminolysis reaction proceeds with its usual chemical mechanism, and (ii) only one enantiomer has antifungal activity. Given the difficulty of single-step chemical strategies for the preparation of chiral fluconazoles in optically enriched form, we anticipate that the enzymatic methodology reported herein will have significant impact in this approach to obtaining novel variants of existing antifungal drugs.

The most active analogue prepared in this study, (-)-*S*-**3d**, is more potent against *Aspergillus fumigatus* than fluconazole, having MIC values of 8-16 µg/mL in a series of *in vitro* assays. Perhaps more importantly for drug discovery, the anti-*Aspergillus* potency of this compound is enhanced (MIC 1.6-4.0 µg/mL) by encapsulation in derivatized nanoparticles, with minimal *in vitro* cytotoxic effects at concentrations of up to 2 mg/mL against human erythrocytes and cell lines of human origin.

Materials and Methods

General procedure for the CAL-B catalysed synthesis of optically enriched fluconazole analogues. CAL-B immobilized on accurel beads (300

219 mg) was added to a solution of the epoxide (\pm)-**1** (5.0 mmol) and the appropriate
220 amine (**2a-j**, **4a** or **4b**, 2.5 mmol) dissolved in THF, and the mixture incubated at 55
221 °C. The extent of the reaction was monitored by TLC and the enzyme was removed
222 by filtration when the amine was consumed. After removal of THF at reduced
223 pressure, the residue was subjected to column chromatography using chloroform/
224 methanol as eluent to afford optically enriched samples of pure fluconazole
225 analogues (-)-**S-3a-3j**, (-)-**S-5a** or (-)-**S-5b** and the unreacted epoxide (+)-**S-1**.

226

227 **(-)-S-2-(2',4'-Difluorophenyl)-1-hexylamino-3-(1'',2'',4'')triazol-1''-yl-prop-**
228 **an-2-ol (3d)** was obtained as a viscous oil in 80% yield. $[\alpha]_D^{20}$ -20.3 (c 0.01,
229 CHCl₃); IR spectrum (film) μ_{\max} : 3315 (OH and NH), 2979, 1620, 1508, 1415, 1267,
230 1145, 960 cm⁻¹. ¹H NMR (400 MHz, CDCl₃): δ 0.83 (3H, t, J = 7.63 Hz), 1.17-1.33
231 (8H, m), 2.43 (2H, t, J = 6.87 Hz), 2.81 (1H, d, J = 12.97 Hz), 3.12 (1H, d, J = 12.21
232 Hz), 4.49 (1H, d, J = 14.50 Hz), 4.58 (1H, d, J = 13.73 Hz), 6.74-6.82 (2H, m), 7.50-
233 7.55 (1H, m), 7.77 (1H, s) and 8.10 (1H, s). ¹³C NMR (100 MHz, CDCl₃): δ 13.92,
234 22.46, 26.55, 29.83, 31.49, 50.00, 54.14 (d, J_{CF} = 3.83 Hz), 55.98 (d, J_{CF} = 4.79 Hz),
235 72.96 (d, J_{CF} = 5.75 Hz), 104.12 (d, J_{CF} = 26.84 Hz), 111.38 (d, J_{CF} = 20.61 Hz), 125.05
236 (d, J_{CF} = 13.42 Hz), 129.79 (d, J_{CF} = 6.71 Hz), 144.60, 151.09, 158.92 (d, J_{CF} =
237 237.78 Hz) and 162.29 (d, J_{CF} = 249.20 Hz). HRMS: m/z 339.1991 ([M+H]⁺,
238 C₁₇H₂₅F₂N₄O calcd. 339.1969).

239

240 **Microbroth dilution assay** Various concentrations of different derivatives in the
241 range of 0.24-1000.0 µg/mL were prepared in 96 well culture plates (Nunc, Roskilde,
242 Denmark) by serial dilution in Sabouraud dextrose broth. Wells were inoculated with
243 1 x 10⁶ spores (conidia) of *Aspergillus* in 10 µL of spore suspension. Negative

controls were solvent in medium and spores only, with amphotericin B and fluconazole being used as positive controls. Plates were incubated at 37 °C using a BOD incubator (Calton, NSW, India) and examined macroscopically after 48 h for the growth of *Aspergillus* mycelia. The activity of the analogues was defined as positive if the medium appeared clear without any growth of *Aspergillus* mycelia, and the minimum concentration of compounds inhibiting growth was reported as MIC (Table 1).

251

Disc diffusion assay Autoclaved Sabouraud dextrose agar (SDA) was poured into radiation-sterilized petri dishes (10.0 cm diameter). A suspension of conidia of *Aspergillus* was prepared and overlaid on the agar plates. Different concentrations of the fluconazole analogues were impregnated on 5.0 mm diameter sterilized discs (Whatman No. 1) and placed on the agar. Control discs containing solvent, amphotericin B or fluconazole were also included in the assay. Plates were incubated at 37 °C and the zone of inhibition determined after 72 h. MICs reported for this assay (Table 1) correspond to fluconazole analogue concentrations giving a zone of inhibition of at least 6.0 mm diameter from the centre of the plate.

261

Percent spore germination inhibition assay Serial dilutions, ranging from 0.24-1000.0 µg/mL, of each fluconazole analogue dissolved in Sabouraud dextrose broth were placed in radiation-sterilized petri dishes (10.0 cm diameter), with each dish then being inoculated with 100 ± 5 *Aspergillus* conidia. After incubation for 16 h at 37 °C, wells were examined for spore germination using an inverted microscope (Nikon Diphot, Japan), and the number of germinated, and non-germinated, spores

268 recorded. MICs in this assay (Table 1) correspond to fluconazole analog
269 concentrations resulting in inhibition of spore germination.

270

271 ***In vitro cytotoxicity assays.*** Two approaches were performed to assess the
272 cytotoxicity of the fluconazole analogues. First, using a standard haemolytic assay
273 [28], erythrocytes from healthy individuals were suspended in phosphate buffered
274 saline (PBS) to give a 2 % suspension (v/v). These cells were then incubated with
275 various concentrations of each compound for 1 h at 37 °C before being pelleted by
276 centrifugation at 3000 x *g* for 10 min. The percentage haemolysis was then
277 calculated from the optical density at 450 nm of the supernatant (Figure 4a). The
278 effect of solvent and PBS on erythrocyte viability was also checked. Triton X-100
279 (Sigma Chemicals, USA) was used for complete haemolysis of the erythrocytes.

280 In an alternate approach, an MTT-based assay [29] was used to examine the
281 cytotoxicity of the analogues against A549 (human pulmonary epithelial cells)
282 and U87 (primary glioblastoma cells) human cell lines, obtained from National
283 Centre for Cell Science, Pune, India (Figures 4b and 4c). Briefly, cells were
284 cultured in RPMI-1640 medium supplemented with L-glutamine and fetal calf
285 serum (10 % v/v), before being harvested at the log phase of confluency and
286 re-suspended in RPMI-1640 medium. Samples (2×10^4 cells in 100 μ L) were
287 seeded into culture plates and allowed to grow overnight at 37 °C under 5 %
288 (v/v) CO₂. Fluconazole analogues were added at a variety of concentrations
289 and the cells were incubated under the same conditions for 24 h. Equivalent
290 amounts of solvent, amphotericin B and fluconazole were used as negative
291 and positive controls. The medium was removed from each well before the
292 addition of 50.0 μ g of 3-(4,5-dimethylthiazol-2-yl)-2,5-diphenyltetrazolium

293 bromide (MTT) in PBS (100 μ L). After incubation for a further period of 4 h at
294 37 °C, the MTT solution was removed and the cells were lysed using
295 isopropanol-HCl (100.0 μ L). The absorption of each well (at 540 nm) was used
296 to determine the percentage cytotoxicity in a micro-plate reader (Spectra max
297 384 plus, Molecular Devices, USA).

298

299 **Acknowledgements**

300 The Council of Scientific and Industrial Research (CSIR, New Delhi), the
301 University of Delhi and the University Grants Commission (UGC, New Delhi)
302 provided research facilities and funding for this study. SM acknowledges the
303 financial support from CSIR, New Delhi through the award of a Senior
304 Research Associateship.

305

306 **References**

- 307 1. **Rousseau N, Picot S, Bienvenu AL.** 2014. Erythropoietin combined with
308 liposomal Amphotericin B improves outcome during disseminated aspergillosis in
309 mice. *Front Immunol* **5**:1-4.
- 310 2. **Arvanitis M, Ziakas PD, Zacharioudakis IM, Zervou FN, Caliendo AM,**
311 **Mylonakis E.** 2014. PCR in diagnosis of invasive aspergillosis: a meta-
312 analysis of diagnostic performance. *J Clin Microbiol* **52**:3731-3742.
- 313 3. **Roemer T, Krysan DJ.** 2014. Antifungal drug development: challenges,
314 unmet clinical needs, and new approaches. *Cold Spring Harb Perspect Med*
315 **4**:1-14.
- 316 4. **McCormick A, Jacobsen ID, Broniszewska M, Beck J, Heesemann J,**
317 **Ebel F.** 2012. The two-component sensor kinase TcsC and its role in stress

- 318 resistance of the human-pathogenic mold *Aspergillus fumigatus*. PLoS One
319 7:e38262.
- 320 5. Yu S, Wang N, Chai X, Wang B, Cui H, Zhao Q, Zou Y, Sun Q, Meng
321 Q, Wu Q. 2013. Synthesis and antifungal activity of novel triazole analogues
322 containing 1,2,3-triazole fragment. Arch Pharm Res 36:1215-1222.
- 323 6. Singh S, Dabur R, Gatne MM, Singh B, Gupta S, Pawar S, Sharma
324 SK, Sharma GL. 2014. *In vivo* efficacy of a synthetic coumarin derivative in a
325 murine model of aspergillosis. PLoS One 9:1-7.
- 326 7. Sanglard D. 2016. Emerging threats in antifungal-resistant fungal pathogens.
327 Front Med doi:10.3389/fmed.2016.00011.
- 328 8. Kumar A, Khan A, Malhotra S, Mosurkal R, Dhawan A, Pandey MK,
329 Singh BK, Kumar R, Prasad AK, Sharma SK, Samuelson LA, Cholli AL,
330 Len C, Richards NGJ, Kumar J, Haag R, Watterson AC, Parmar VS. 2016.
331 Synthesis of macromolecular systems via lipase catalyzed biocatalytic
332 reactions: Applications and future perspectives. Chem Soc Rev 45:6855-
333 6887.
- 334 9. Gandhi NN, Patil NS, Sawant SB, Joshi JB, Wangikar PP, Mukesh D.
335 2000. Lipase-catalyzed esterification. Catal Rev 42:439-480.
- 336 10. Kumar R, Chen MH, Parmar VS, Samuelson LA, Kumar J, Nicolosi
337 R, Yoganathan S, Watterson AC. 2004. Supramolecular assemblies based
338 on copolymers of PEG 600 and functionalized aromatic diesters for drug
339 delivery applications. J Am Chem Soc 126:10640-10644.

- 340 11. **Malhotra S, Calderón M, Prasad AK, Parmar VS, Haag R.** 2010. Novel
341 chemoenzymatic methodology for the regioselective glycine loading on
342 polyhydroxy compounds. *Org Biomol Chem* **8**:2228-2237.
- 343 12. **Bhatia S, Mohr A, Mathur D, Parmar VS, Haag R, Prasad AK.** 2011.
344 Biocatalytic route to sugar-PEG-based polymers for drug delivery
345 applications. *Biomacromolecules* **12**:2543-2555.
- 346 13. **Tett S, Moore S, Ray J.** 1995. Pharmacokinetics and bioavailability of
347 fluconazole in two groups of males with human immunodeficiency virus (HIV)
348 infection compared with those in a group of males without HIV infection.
349 *Antimicrob Agents Chemother* **39**:1835-1841.
- 350 14. **Lass-Flörl C.** 2011. Triazole antifungal agents in invasive fungal infections: A
351 comparative review. *Drugs* **71**:2405-2419.
- 352 15. **Karthauss M.** 2011. Prophylaxis and treatment of invasive aspergillosis with
353 voriconazole, posaconazole and caspofungin - review of the literature. *Eur J*
354 *Med Res* **16**:145-152.
- 355 16. **Yamada H, Tsuda T, Watanabe T, Ohashi M, Murakami K, Mochizuki H.**
356 1993. *In vitro* and *in vivo* antifungal activities of D0870, a new triazole agent.
357 *Antimicrob Agents Chemother* **37**:2412-2417.
- 358 17. **Young-Min N.** 2011. Synthesis and activity of novel 1-halogenbenzylindole
359 linked triazole analogues as antifungal agents. *Bull Korean Chem Soc*
360 **32**:307-310.
- 361 18. **Pore VS, Jagtap MA, Agalave SG, Pandey AK, Siddiqi MI, Kumar V,**
362 **Shukla PK.** 2012. Synthesis and antifungal activity of 1, 5-disubstituted-1, 2,
363 3-triazole containing fluconazole analogues. *MedChemCommun* **3**:484-488.

- 364 19. **Borate HB, Sawargave SP, Chavan SP, Chandavarkar MA, Iyer RR,**
365 **Nawathye VV, Chavan GJ, Tawte AC, Rao DD.** 2012. Enantiomers of
366 fluconazole analogues containing thieno-[2,3-d]pyrimidin-4(3h)-one moiety as
367 antifungal agents. PCT Int Appl: WO 2012123952 A1.
- 368 20. **Yang J, Han S, Zheng H, Dong H, Liu J.** 2015. Preparation and application
369 of micro/nanoparticles based on natural polysaccharides. Carbohydr Polym
370 **123**:53-66.
- 371 21. **Chai X, Zhang J, Yu S, Hu H, Zou Y, Zhao Q, Dan Z, Zhang D, Wu Q.**
372 2009. Design, synthesis and biological evaluation of novel 1-(1*H*-1,2,4-
373 triazole-1-yl)-2-(2,4-difluorophenyl)-3-substituted benzylamino-2-propanols.
374 Bioorg Med Chem Lett **19**:1811-14.
- 375 22. **Zhao Q, Song Y, Hu H, Sun Q, Zhang J, Wu Q.** 2006. Synthesis of α -(2,4-
376 difluorophenyl)- α -(1*H*-1,2,4-triazol-1-ylmethyl)-1-piperidineethanol analogues
377 and determination of their activity as antifungal agents. Zhongguo Yaowu
378 Huaxue Zazhi **16**:150-153.
- 379 23. **Saksena AK, Girjavallabhan VM, Lovey RG, Pike RE, Desai JA, Ganguly**
380 **AK, Hare RS, Loebenberg D, Cacciapuoti A, Parmegiani RM.** 1994.
381 Enantioselective synthesis of the optical isomers of broad-spectrum orally
382 active antifungal azoles, Sch 42538 and Sch 45012. Bioorg Med Chem Lett
383 **4**:2023-2028.
- 384 24. **Dabur R, Sharma GL.** 2002. Studies on antimycotic properties of
385 *Daturametel*. J Ethnopharmacol **80**:193-197.

- 386 25. **Yadav V, Mandhan R, Dabur R, Chhillar AK, Gupta J, Sharma GL.** 2005.
387 A fraction from *Escherichia coli* with anti-*Aspergillus* properties. J Med
388 Microbiol **54**:375-379.
- 389 26. **Dabur R, Chhillar AK, Yadav V, Kamal PK, Gupta J, Sharma GL.** 2005. *In*
390 *vitro* antifungal activity of 2-(3,4-dimethyl-2,5-dihydro-1H-pyrrol-2-yl)-1-
391 methylethyl pentanoate, a dihydropyrrole derivative. J Med Microbiol **54**:1-4.
- 392 27. **Yoo JW, Doshi N, Mitragotri S.** 2011. Adaptive micro and nanoparticles:
393 temporal control over carrier properties to facilitate drug delivery.
394 Adv Drug Deliv Rev **63**:1247-1256.
- 395 28. **Latoud C, Peypoux F, Michel G, Genet R, Morgat JL.** 1986. Interactions of
396 antibiotics of the iturin group with human erythrocytes. Biochim Biophys Acta
397 **856**: 526-535.
- 398 29. **Mossman T.** 1983. Rapid colorimetric assay for cellular growth and survival:
399 application to proliferation and cytotoxicity assays. J Immunol Methods **65**:
400 55-63.

401 **Figure Captions**

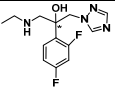
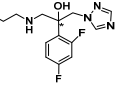
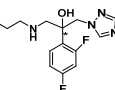
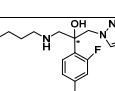
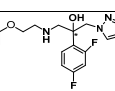
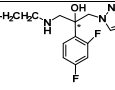
402 **Figure 1.** CAL-B catalyzed epoxide ring opening with open chain and cyclic aliphatic
403 amines. Note that samples of each compound could also be prepared in racemic
404 form by heating the epoxide and amine at 55 °C in THF (see Supporting
405 Information). The new stereogenic centre is indicated by an asterisk.

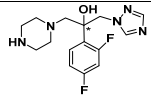
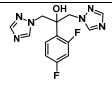
406 **Figure 2.** *In vitro* release of (-)-**S-3d** from *O*-hexadecyl- (blue triangles), *O*-decyl-
407 (red circles) and *O*-heptyl-derivatized (grey squares) dextran nanoparticles.

408 **Figure 3.** *In vitro* antifungal activity of (-)-**S-3d**, amphotericin B and their
409 dextran NPs. Lane a: Negative control; Lane b: Empty *O*-alkyl dextran
410 nanoparticles; Lane c: Amphotericin B; Lane d: Fluconazole; Lane e: (-)-**S-3d**;
411 Lane f: *O*-heptyl nanoparticles containing (-)-**S-3d**; Lane g: *O*-decyl
412 nanoparticles containing (-)-**S-3d**; Lane h: *O*-hexadecyl nanoparticles
413 containing (-)-**S-3d**; Lane i: *O*-heptyl nanoparticles containing Amphotericin B;
414 Lane j: *O*-decyl nanoparticles containing Amphotericin B; Lane k: *O*-hexadecyl
415 nanoparticles containing Amphotericin B.

416 **Figure 4.** *In vitro* cytotoxicity assays for optically enriched (-)-**S-3d** and amphotericin
417 B in both the free form and when encapsulated into dextran nanoparticles. (a)
418 Haemolytic assay; MTT-based assay using (b) A459 and (c) U87 cell lines.

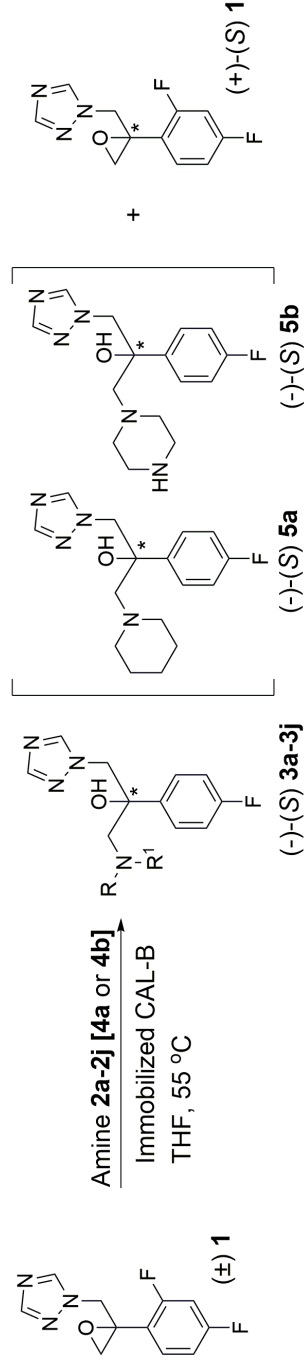
Table 1: *In vitro* activity of selected, optically enriched fluconazole analogues against *Aspergillus* species.^{a,b}

	Analogue	<i>Aspergillus fumigatus</i>			<i>Aspergillus niger</i>			<i>Aspergillus flavus</i>		
		MDA ($\mu\text{g/ml}$)	DDA ($\mu\text{g/disc}$)	PSGI ($\mu\text{g/ml}$)	MDA ($\mu\text{g/ml}$)	DDA ($\mu\text{g/disc}$)	PSGI ($\mu\text{g/ml}$)	MDA ($\mu\text{g/ml}$)	DDA ($\mu\text{g/disc}$)	PSGI ($\mu\text{g/ml}$)
(-)- S-3a		125.0 (250.0)	62.50 (125.0)	125.0 (250.0)	250.0 (250.0)	125.0 (125.0)	250.0 (250.0)	250.0 -	125.0 -	250.0 -
(-)- S-3b		250.0 (250.0)	62.50 (125.0)	250.0 (250.0)	500.0 -	125.0 -	500.0 -	- -	- -	- -
(-)- S-3c		62.50 (125.0)	31.25 (31.25)	62.50 (125.0)	62.50 (500.0)	31.25 (125.0)	62.50 (500.0)	500.0 (1000.0)	125.0 (125.0)	500.0 (1000.0)
(-)- S-3d		15.62 (15.62)	7.81 (7.81)	15.62 (15.62)	62.50 (125.0)	15.62 (31.25)	62.50 (125.0)	125.0 (125.0)	15.62 (31.25)	125.0 (125.0)
(-)- S-3e		62.50 (125.0)	31.25 (62.50)	62.50 (125.0)	125.0 (500.0)	62.50 (125.0)	125.0 (500.0)	500.0 (500.0)	125.0 -	500.0 (500.0)
(-)- S-3i		500.0 (500.0)	250.0 (250.0)	500.0 (500.0)	500.0 -	125.0 -	500.0 -	500.0 -	250.0 -	500.0 -

(-)-S-5b		62.50 (125.0)	31.25 (62.50)	62.50 (125.0)	125.0 (500.0)	62.50 (125.0)	125.0 (500.0)	500.0 (500.0)	125.0 (125.0)	500.0 (500.0)
	 Fluconazole	250.0	125.0	250.0	250.0	125.0	250.0	250.0	125.0	250.0
	Amphotericin B	1.95	0.97	1.95	1.95	0.97	1.95	1.95	0.97	1.95

^aValues in parentheses are for the racemic form of the compound.

^b(-) shows no activity within the range of concentrations tested.



- 2a or 3a:** R = H, R' = CH₂CH₃
2b or 3b: R = H, R' = CH₂CH₂CH₃
2c or 3c: R = H, R' = CH₂(CH₂)₂CH₃
2e or 3e: R = H, R' = CH₂CH₂OPh
2f or 3f: R = CH₃, R' = CH₂(CH₂)₁₆CH₃
2g or 3g: R = H, R' = CH₂(CH₂)₂N(CH₃)₂
2h or 3h: R = H, R' = CH₂(CH₂)₂N(CH₂CH₃)₂
2i or 3i: R = H, R' = CH₂CH₂Ph
2j or 3j: R = H, R' = CH₂(CH₂)₂CH₂Ph

